Purification and Characterization of the *Caenorhabditis elegans* HCF Protein and Domains of Human HCF†

Bi-Tzen Juang,‡ Ander Izeta,§ Peter O'Hare,§ and Ben F. Luisi*,‡

Department of Biochemistry, University of Cambridge, 80 Tennis Court Road, Cambridge CB2 1GA, U.K., and Marie Curie Research Institute, The Chart, Oxted, Surrey RH8 OTL, U.K.

Received February 25, 2005; Revised Manuscript Received May 16, 2005

ABSTRACT: The human cellular factor (HCF) is a multidomain protein that is implicated in processes of cell cycle progression, and it is recruited into a multicomponent assembly that triggers the expression of the herpes simplex virus genome. The amino-terminal domain of HCF has been proposed to form a "kelch" type β-propeller fold, and the carboxy-terminal domain contains a repeat of a fibronectin-like motif. We describe the expression, purification, and characterization of the domains from the human HCF and of the full-length HCF from *Caenorhabditis elegans.* The purified recombinant *C. elegans* HCF can substitute for the human HCF in efficiently forming a multiprotein complex on a herpes simplex virus promoter element. As noted in earlier studies, a segment of human HCF encompassing the human kelch domain forms a stable complex on a viral promoter element. The purified fibronectin domain can also be recruited into this complex, but not into the stable complex formed with the minimal kelch domain. These results suggest that the fibronectin domain can interact with HCF in the transcriptional activating complex and that the association requires a region outside the putative β-propeller.

The human nuclear protein HCF-1 was originally identified as a transcriptional coactivator involved in gene expression of the herpes simplex virus (HSV).[1] After viral infection, the viral transcriptional activator VP16 (also termed Vmw65 and αTIF) forms a heteromeric complex with HCF-1 (also called C1, VCAF, and CFF). The complex then recruits the cellular DNA-binding protein, Oct-1, on the TAATGA(G/A)AT element in the upstream promoter of the HSV viral immediate-early genes, and activates transcription (reviewed in ref *2*). In addition to its role in the activation of viral genes, HCF-1 acts as a vehicle for nuclear import of VP16. This activity requires a nuclear localization signal (NLS) located at the C-terminus of HCF-1 (*3*).

The 380 amino-terminal residues of HCF-1 were shown to be sufficient to bind VP16, stabilize the VP16-induced complex, and activate transcription in vivo (*4*, *5*). Examination of the sequence of these amino-terminal residues reveals six copies of a sequence motif that was first defined in the *Drosophila* protein kelch (*6*). This kelch-like region has been proposed to have a β-propeller structure, whereby the "blades" of the propeller are made of at least four antiparallel β-strands, and six such blades form a self-closing barrel-like architecture (reviewed in ref *7*).

The domain organization of HCF-1 is shown in Figure 1. HCF-1 is synthesized as a large polypeptide of 2035 amino acids and is subsequently processed by proteolytic cleavage at a series of six HCF-1_{PRO} repeats located near the center of the protein (*8*−*10*). This processing generates two domains that are associated noncovalently through the interaction of two sets of "self-association sequence": SAS1N pairs with SAS1C, and SAS2N pairs with SAS2C (*11*). The SAS1C domain corresponds to a pair of fibronectin type 3 (FnIII) sequence motifs, and this domain interacts with a 43-residue sequence (SAS1N) outside the kelch domain at the N-terminus. The FnIII motif is predicted to form a globular domain with layered β-sheets, like that found repetitively in fibronectin and other cell surface proteins. The SAS2 domains are located in basic and acidic regions and have been mapped with less precision. Predictive methods indicate that these SAS2 regions may not be structured.

A number of potential cellular partners of HCF-1 have been identified. For instance, the kelch domain associates with two basic-leucine zipper transcription factors LZIP (or Luman) and Zangfei and a cellular nuclear export factor HPIP (*12*−*16*). In the basic, acidic, and NLS regions, the interacting proteins include Sp1, GA-binding protein (GABPβ), Miz-1, protein phosphatase 1, and the programmed cell-death protein PDCD2 (*17*−*21*). Last, a methyltransferase and a deactylase, both involved in histone modification, have been found to associate with the N-terminus of HCF-1, indicating that HCF-1 might regulate gene expression through the

† This work was supported by the Wellcome Trust.

* To whom correspondence should be addressed. E-mail: ben@cryst.bioc.cam.ac.uk. Phone: 44-1223-766019. Fax: 44-1223-766002.

‡ University of Cambridge.

§ Marie Curie Research Institute.

[1] Abbreviations: HCF, human cellular factor; HCF-1(N380), HCF-1(N411), and HCF-1(C1772), derivatives of the human HCF-1 protein corresponding to residues 2−380, 2−411, and 1772−2005, respectively; CeHCF, *C. elegans* human cellular factor homologue; VP16, viral protein 16, also known as α-TIF, Vmw65; VIC, VP16-induced complex comprising Oct-1, HCF, VP16, and the herpes simplex virus promoter element; HSV, herpes simplex virus; NLS, nuclear localization signal; FnIII, fibronectin type III sequence motif.

10.1021/bi050357l CCC: $30.25
Published on Web 07/02/2005

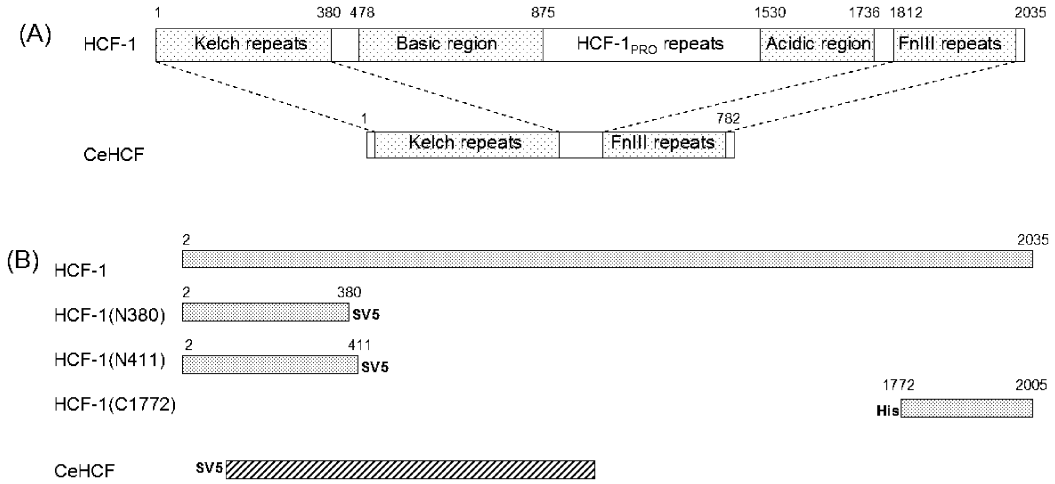

FIGURE 1: Domain organization of human HCF-1 and *C. elegans* HCF. (A) Full-length HCF-1 and *C. elegans* HCF (CeHCF) are illustrated with structural and functional domains indicated. (B) Summary of HCF constructs studied here: HCF-1(N380), HCF-1(N411), HCF-1(C1772), and full-length CeHCF. The affinity tags, SV5 and poly-His, are indicated at either the N-terminus or the C-terminus.

modulation of chromatin structure (*22*). The precise role of these myriad interactions in the cellular function of HCF remains unclear.

Although information about HCF-1 cellular function may be incomplete, HCF-1 has been shown to be required for normal cell proliferation. In particular, a point mutation has been identified in the HCF-1 kelch domain that is associated with cell cycle arrest at G0/G1 with elevated temperature, suggesting that HCF-1 is likely to play an important role in cell cycle progression (*23*, *24*). Further analysis of this mutant implicates the kelch domain in the entry into the cell cycle, and the fibronectin domain in the cytokinesis required for exit from the cycle (*25*).

Human cells contain a shorter paralogue of HCF-1, known as HCF-2. This protein is also composed of six kelch repeats and a C-terminal FnIII domain, but the central region lacks the HCF_{PRO} repeats that characterize HCF-1 (*26*). The HCF counterpart in the worm *Caenorhabditis elegans* (CeHCF) is very similar in size and domain organization to HCF-2, and it too lacks the HCF_{PRO} region (*27*). Neither HCF-2 nor CeHCF undergoes proteolytic processing. Both HCF-2 and CeHCF can support VP16-induced complex formation in vitro (*27*, *28*). However, the VP16-induced complex containing CeHCF can activate transcription, whereas HCF-2 supports comparatively little transcription (*26*, *28*). Like human HCF-1, the C-terminal region of CeHCF contains a nuclear localization signal (*29*).

To study the structure and function of HCF, we produced the kelch domain of HCF-1 and the full-length CeHCF in soluble form using a *Drosophila* embryo cell line. A series of chromatographic separations was performed, and we demonstrate that the purified CeHCF can support VP16-induced complex formation in the presence of bacterially expressed VP16 and Oct-1 proteins. We also describe here the expression, purification, and biophysical characterization of the FnIII repeats of HCF-1 produced in bacteria. The purified FnIII domain is co-recruited in a VP16-dependent complex on viral DNA together with a segment of HCF-1 encompassing both the kelch domain and the SAS1 region. These results suggest that the interdomain interactions of HCF-1 may be maintained in the transcriptional activating complex.

EXPERIMENTAL PROCEDURES

Construction of Expression Plasmids

An KpnI/XbaI fragment from the mammalian expression vector, pSM8 encoding full-length *C. elegans* HCF (CeHCF) with an SV5 tag at the N-terminal end, was inserted into the *Drosophila* expression plasmid, pMT/V5-His (Invitrogen).

The gene encoding the N-terminal kelch domain (amino acids 2−380) of human HCF-1 [HCF-1(N380)] was generated by PCR from the plasmid pTH1 (*30*), encoding human HCF-1 (residues 2−491) using the following forward and reverse primers: 5′-TTCGAATTCACC*ATG*GCTTCGGCCGTGTCGCCCGC-3′ and 5′-CCGCTCGAGCAGGGAGTTGGTGTTGGCGCGTAC-3′ (restriction enzyme sites, EcoRI and XhoI, are underlined; the start codon is shown in italics). The amplified fragments were treated with the restriction enzymes and ligated into pMT/V5-His containing the C-terminal SV5 epitope. Human HCF-1 {amino acids 2−411 [HCF-1(N411)]} was constructed by the same procedure described above, substituting for the reverse primer the 5′-ACTGAGCTCTCAGTGGTGGTGGTGGTGGTGCTCGAGGGAGGTGGCAGTAGCAGCCG-3′ oligonucleotide (a restriction enzyme site, XhoI, is underlined).

To create the expression vector for the C-terminal fibronectin type III-like domain of human HCF-1, the coding sequence {amino acids 1772−2005 [HCF-1(C1772)]} was generated by PCR from pCGNHCF that contained full-length HCF-1 using the following oligonucleotides primers: 5′-GGATCCCAT*ATG*CCAGCCAAGCTGCAGGCTGCA-3′ and 5′-CTCGAGCATATG**TCA**TTTACTGGTTTCCTGCAGCCACCTCAC-3′ (restriction enzyme sites, NdeI, are underlined; the start codon is shown in italics; the stop codon is shown in bold). The product was subcloned into an *Escherichia coli* T7 expression vector, pET28a (Novagen) with the N-terminal His tag. All constructs were confirmed by DNA sequencing.

Cell Culture

Plasmids (19 μg) encoding the full-length CeHCF and 1 μg of selective vectors (pCoHYGRO) (Invitrogen) were cotransfected into Schneider cells (S2; 3×10^6 cells) by the

calcium phosphate transfection method (Invitrogen). Stable transfectants were selected in the presence of hygromycin-B (Sigma) at 300 μg/mL for approximately 3 weeks. Selected cells were maintained in complete *Drosophila* expression medium [10% heat-inactivated FBS (Sigma) and 1% penicillin and streptomycin (Sigma) in Schneider's *Drosophila* medium (Gibco)] at a density of $1-10 \times 10^6$ cells/mL at 22−24 °C. For large-scale expression (2−6 L), the cells were grown in an Erlenmeyer shaker flask (Corning) in complete *Drosophila* expression medium with 0.1% Pluronic F-68 (Sigma) at 25−27 °C. Protein expression was induced with 0.5 mM $CuSO_4$ for 24−48 h at a cell density of $5-10 \times 10^6$ cells/mL.

Purification of Recombinant C. elegans HCF Expressed in Drosophila Cell Culture

S2 cell nuclear extracts were prepared following the procedure of Gay et al. (*31*). S2 cell culture was harvested at a density of $5-10 \times 10^6$ cells/mL. All purification procedures were performed at 4 °C. The cells were resuspended in 1/80 volume of ice-cold buffer A [15 mM HEPES (pH 7.6), 10 mM KCl, 5 mM $MgCl_2$, 0.1 mM EDTA, 1 mM DTT, and protease inhibitors (Roche)] and then spun at 1000*g* for 10 min. The cell pellets were resuspended in buffer A and lysed with 25 strokes of a Dounce type B pestle. The nuclei were collected by spinning, and the supernatant, corresponding to cytoplasm portions, was stored at −80 °C for further purification. The nuclear pellets were resuspended in buffer A, adjusted to 150 mM KCl, and lysed by the addition of ammonium sulfate to a final concentration of 400 mM. The nuclear lysates were centrifuged at 120000*g* for 1 h, and the soluble proteins in the supernatant were precipitated by the addition of 60% saturated ammonium sulfate. The precipitate was redissolved in 25 mM HEPES (pH 7.6), 100 mM KCl, 5 mM $MgCl_2$, 0.1 mM EDTA, 1 mM DTT, 20% (v/v) glycerol, and complete protease inhibitor tablets (Roche). The supernatant was stored at −80 °C.

Proteins were isolated from a large-scale preparation of S2 cell nuclear extracts and cytoplasm by the following purification procedures.

Step 1. Immobilized Heparin Chromatography. A HiTrap heparin column (5 mL; Amersham) was pre-equilibrated with buffer B [25 mM HEPES (pH 7.6), 1 mM EDTA, 50 mM NaCl, 1 mM DTT, 10% (v/v) glycerol, and protease inhibitors] and loaded with nuclear extract (40−80 mg of protein). The column was washed with 5 column volumes of buffer B, and then HCF was eluted with 25 mL of a linear gradient from 0.05 to 2 M NaCl at a flow rate of 1 mL/min. All eluants were analyzed by immunoblot analysis and mobility shift assay (see below). The peak fractions (approximately 10 mL) were desalted using HiPrep 26/10 desalting columns (Amersham) equilibrated with buffer.

Step 2. Ion-Exchange Chromatography. The appropriate fractions from step 1 were pooled and loaded onto a Mono Q column (HR 5/5, Amersham) pre-equilibrated with buffer B, washed with 5−10 column volumes of buffer B, and then eluted with 50 mL of a linear gradient from 0.05 to 1 M NaCl followed by 5 mL of 1 M NaCl. The flow-through fractions from nuclear extracts were applied onto a Mono S column (HR 5/5, Amersham) and followed by the same procedure described above. Fractions containing the peak of HCF activity were combined and concentrated to 0.5−1 mL using vivaspin 20 concentrators [30 000 molecular weight cutoff (MWCO), Vivascience] at 5000*g* and 4 °C.

Step 3. Size-Exclusion Chromatography. The concentrated samples from step 2 were loaded onto a Superdex 200 column pre-equilibrated with buffer C [25 mM HEPES (pH 7.6), 0.2 mM EDTA, 100 mM KCl, 0.5 mM DTT, 5% (v/v) glycerol, and protease inhibitors]. The samples were eluted with the same buffer at a flow rate of 0.5 mL/min.

Step 4. Affinity Column. The eluants from step 3 were combined and incubated for 10−12 h with anti-V5 agarose affinity gel (Sigma) prewashed with buffer D [20 mM HEPES (pH 7.6), 20% (v/v) glycerol, 0.2 mM EDTA, 0.1% (v/v) Triton X-100, and protease inhibitors]. After incubation, the gel was washed five times with buffer D containing 100 mM KCl and five times with buffer D containing 10% (v/v) glycerol and 100 mM NaCl. The CeHCF was eluted by incubating the beads with buffer D containing 10% (v/v) glycerol, 100 mM NaCl, and 0.2 mg/mL V5 peptide (Sigma). This elution step was carried out at room temperature, and each incubation step was performed for 20 min. The eluants were combined, concentrated with a vivaspin 0.5 mL concentrator (30 000 MWCO PES, Vivascience), and analyzed by SDS−PAGE and immunoblotting. Protein activity was monitored by the mobility shift assay.

Production and Purification of the C-Terminal Fibronectin Type III-like Domain of Human HCF-1

Expression constructs were transformed into *E. coli* strain codon bias-adjusted BL21(DE3). The bacterial culture was grown in LB medium to an A_{600} of 0.6−0.8 at 37 °C, induced with 0.5 mM IPTG, and then continuously incubated for 2−3 h at 37 °C before being harvested. Cells were pelleted and frozen at −80 °C. After thawing on ice, cell pellets were resuspended in 1/20 culture volume of ice-cold buffer E [50 mM Na_2HPO_4 (pH 7.4), 300 mM NaCl, 20% (v/v) glycerol, 10 mM imidazole (pH 7.5), and protease inhibitors] and sonicated with four applications of 15 s pulses on ice (XL2020 Ultrasonic Liquid Processor, Misonix). Cell debris was pelleted at 30000*g* for 30 min at 4 °C, and the supernatant was collected for further purification. The following procedures were performed at room temperature.

Step 1. Immobilized Metal Chromatography. A HiTrap Chelating column (5 mL; Amersham) was charged with 0.1 M Ni_2SO_4 and then pre-equilibrated with buffer E. Bacterial lysates from a 0.5−1 L culture were applied. The column was washed with 5 column volumes of buffer E, and then the HCF fibronectin-like domain was eluted with 50 mL of a linear gradient from 0.01 to 0.5 M imidizole at pH 7.5. All eluants were analyzed by SDS−PAGE, and the peak fractions were desalted using a HiPrep 26/10 desalting column equilibrated with buffer F [20 mM KH_2PO_4 (6.6), 1 mM EDTA, 1 mM DTT, and 5% (v/v) glycerol].

Step 2. Ion-Exchange Chromatography. The pooled, enriched eluant from step 1 was applied onto a HiTrap SP HP column (5 mL; Amersham) pre-equilibrated with buffer E, washed with 3 column volumes of buffer F, and then eluted with 50 mL of a linear gradient from 0 to 0.60 M NaCl followed by 5 mL of a sharp linear gradient from 0.6 to 2 M NaCl. Fractions containing HCF were combined and concentrated to 2−4 mL using vivaspin 20 concentrators (5000 MWCO) at 5000*g* and 4 °C.

Step 3. Size-Exclusion Chromatography. The concentrated proteins from step 2 were further fractionated using a Superdex 75 column (Amersham) pre-equilibrated with buffer G [20 mM KH_2PO_4 (pH 6.6) and 200 mM NaCl]. Protein purity was monitored by SDS−PAGE. Typically, ~2−3 mg of fusion protein was obtained per liter of induced culture.

HCF Localization

All of following steps were carried out at room temperature. The overnight-induced *Drosophila* S2 cells at a density of 2×10^6 cells/mL were settled to a chamber slide that was treated with 0.01% (v/v) poly-L-lysine. The attached cells were incubated with a fixative [PBS, 3.7% (v/v) formaldehyde, and 0.1% (v/v) Nonidet P-40] for 15 min. After the fixative had been removed, the cells were rinsed with PBN (PBS and 0.1% Nonidet P-40). The chamber slides were blocked with PBN containing 10% (w/v) dried nonfat milk for 30 min. Mouse monoclonal anti-SV5 antibody (a kind gift of R. Randall, University of St. Andrews, St. Andrews, U.K.) was used as a primary antibody and diluted 1:10000 in PBN containing 1% nonfat milk. The cells were incubated with 500 μL of the diluted antibody for 1 h and then rinsed three times with PBN for 5 min each. Secondary antibodies, fluorescently labeled with Alexa 488 (Molecular Probes), were also diluted 1:200 in PBN containing 1% (w/v) milk, and 500 μL was applied to a chamber slide for 1 h. The cells were washed three times with PBN. Chamber slides were mounted with Mowiol 40-88 (Aldrich) in the presence of 0.1 mg/mL propidium iodide (Sigma). Dual-channel fluorescence images were acquired on a Zeiss LSM410 laser scanning confocal microscope with separate sequential scanning for each channel.

Western Blotting

Samples were separated by SDS−PAGE and electrotransferred to PVDF membranes. Membranes were soaked in blocking buffer [0.2% (w/v) dry nonfat milk, 0.1% (v/v) Tween 20, and 2 mM azide] overnight and then washed with TTBS [100 mM Tris-HCl (pH 7.5), 0.4% (w/v) NaCl, and 0.1% (v/v) Tween 20]. The membranes were probed with monoclonal anti-SV5 antibody containing horseradish peroxidase conjugate (Invitrogen) and detected using ECL Western blot detection reagents (Amersham Pharmacia).

Pull-Down Assays

The CeHCF fractions from size-exclusion chromatography were incubated with affinity agarose beads pre-equilibrated with buffer [20 mM HEPES (pH 7.6), 10% (v/v) glycerol, 0.2 mM EDTA, 100 mM KCl, 0.5 mM DTT, and protease inhibitors] at 4 °C overnight. The beads were then washed five times in the same buffer, then loaded on a SDS−PAGE gel, and analyzed by Western blotting using an anti-V5 antibody.

Analysis of Recombinant HCF Binding Activity Using an Electrophoretic Mobility Shift Assay

VP16 and the Oct-1 POU domain were prepared as described by Grossmann et al. (*32*) and Chang et al. (*33*). To assay the HCF activity, the reaction mixture (final volume of 20 μL) contained 0.1 μg of VP16, 5 ng of the Oct-1 POU domain, and test HCF samples in binding buffer [25 mM HEPES (pH 7.9), 50 mM NaCl, 10% (v/v) glycerol, 200 μg/mL bovine serum albumin, 0.05% (v/v) NP40, 1 mM DTT, 1 mM EDTA, and 1 μg of poly(dI·dC)]. After a 10 min incubation at room temperature, 1 μL of end-labeled oligonucleotide probe 5′-CCATGGAGATCTCGTGCATGCTAATGATATTCTT-3′ was added to the mixture and incubation continued for a further 30 min. Samples were then loaded onto 8% nondenaturing acrylamide gels (39:1 acrylamide:bisacrylamide ratio). Electrophoresis was performed at room temperature for 4 h at 200 V in a buffer containing 0.5× TBE buffer. After being dried, the gels were exposed on phosphor screens overnight and the signal was detected using the FX molecular imager (Bio-Rad).

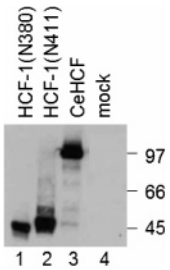

FIGURE 2: Expression of HCF in *Drosophila* S2 cells. Western blot analysis of two truncated HCF-1 kelch domains and full-length CeHCF. Cells were transfected with plasmids expressing the SV5−HCF protein, and stable transfectants were selected. The cell lysates from induced cultures were analyzed with SV5 antibodies.

RESULTS

Expression and Subcellular Localization of HCF in Drosophila S2 Cells. The isolated N-terminal region [amino acids 1−380, hereafter HCF-1(N380)] of HCF-1 is sufficient for formation of a VP16-induced complex (*4*) (Figure 1). As this domain contains the kelch repeats, it might be expected to form an autonomously folding β-propeller structured domain; however, we found that the production of HCF-1(N380) was poor or yielded inclusion bodies using bacterial expression systems (data not shown). The slightly larger expression constructions encoding the first 411 residues of HCF-1 [HCF-1(N411)] also failed to express soluble proteins in *E. coli*. Despite exhaustive attempts, we were unable to refold these denatured proteins.

Given the poor yields and insolubility of HCF prepared with bacterial expression systems, we explored eukaryotic systems to prepare the functional protein. Our efforts with *Saccharomyces cerevisiae* and *Pichia pastoris* as hosts and using a variety of inducible vectors did not yield detectable amounts of protein, but we could successfully express the β-propeller domain of human HCF-1 and full-length CeHCF using the *Drosophila* Schneider S2 cell line. The coding sequences for HCF-1(N380), HCF-1(N411), and full-length CeHCF were cloned into *Drosophila* S2 expression plasmids in-frame with an SV5 epitope. Using Western blotting, HCF-1(N380) and HCF-1(N411) were detected as bands of the expected mass in cell lysates from stable polyclonal transfectants (Figure 2A, lanes 1 and 2). For CeHCF, a major band (90 kDa) was observed, consistent with full-length CeHCF, together with a variable amount of small products, likely representing nonspecific breakdown products (Figure 2A, lane 3).

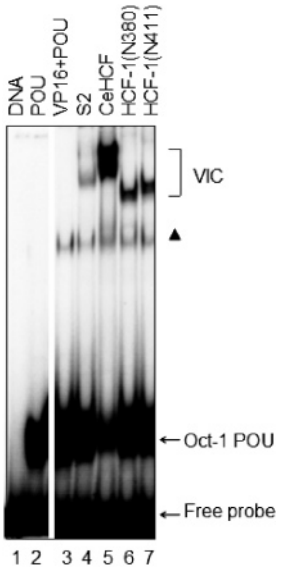

FIGURE 3: Recombinant HCF supports VP16-induced complex formation. Proteins were expressed in S2 cells and tested for VP16-induced complex forming activity with an electrophoretic mobility shift assay. The first four lanes were controls showing the probe alone (lane 1), the Oct-1 POU domain alone (lane 2), the Oct-1 POU domain mixed with VP16 (lane 3), and S2 cell lysates mixed with the Oct-1 POU domain and VP16 (lane 4). In the remaining lanes, lysates expressing CeHCF (lane 5), HCF-1(N380) (lane 6), and HCF-1(N411) (lane 7) were mixed with the Oct-1 POU domain and VP16. Positions of the free probe, the Oct-1 POU domain complex, and the VP16-induced complex (VIC) are indicated. Weaker complexes, likely to represent an Oct-1−VP16 association on the DNA, are indicated with a triangle.

To determine the location of HCF in *Drosophila* S2 cells, the induced cells were analyzed by immunofluorescence. In all cells that expressed full-length CeHCF, the fluorescence was located predominantly in the nucleus, whereas two truncated HCF-1 proteins were located in the cytoplasm (results not shown).

Recombinant C. elegans HCF from the Drosophila Cell Culture Is Able To Form a VP16-Induced Complex. To determine whether truncated recombinant HCF-1 proteins and full-length CeHCF produced in *Drosophila* S2 cells were capable of supporting VP16-induced complex formation, these proteins were tested in electrophoretic mobility shift assays. Equal amounts of whole cell extracts from cells expressing the HCFs were incubated with recombinant VP16 and Oct-1 POU domain proteins, both synthesized in *E. coli*, and a ^{32}P-labeled oligonucleotide probe containing a TAATGAAAT motif. Complexes were separated by electrophoresis on nondenaturing gels (Figure 3).

The independent binding of the POU domain to the DNA probe is shown in lane 2 of Figure 3. The POU domain and VP16 did not form a complex in the absence of HCF (lane 3). (Note that an additional band seen in lanes 3−7 most likely represents a weaker Oct-1−VP16 complex on the DNA.) In the presence of whole cell extracts from cells expressing CeHCF, HCF-1(N380), and HCF-1(N411) (lanes 5−7), supershifted species were observed which we will call "VP16-induced complexes" (VICs). Additional controls showed that the VICs were not formed when either the POU domain or VP16 was omitted (data not shown). The addition of control *Drosophila* S2 cell extracts to VP16 and POU domain resulted in a low level of VIC that is most likely formed by endogenous *Drosophila* HCF (lane 4). These gel mobility results suggest that the CeHCF, HCF-1(N380), and HCF-1(N411) proteins produced in *Drosophila* S2 cells are each functionally active.

Large-Scale Expression, Purification, and Functional Assay of Soluble C. elegans HCF. For large-scale expression of HCF, the transfected S2 cell cultures were prepared as described in Experimental Procedures. To purify CeHCF, we used a series of sequential steps involving immobilized heparin chromatography, followed by ion-exchange, size-exclusion, and affinity chromatographies. For the first step, the nuclear extracts and cytoplasmic proteins were separated from the induced S2 cells and loaded on a heparin column. The fractionation and activity of CeHCF were analyzed by Western blotting and a mobility shift assay (Figure 4). Surprisingly, analysis of the material showed that ~90% of the detectable CeHCF from the nuclear extracts was in the flow-through of the heparin or ion-exchange columns, whereas CeHCF in the cytoplasm was mostly retained on these columns (data not shown). This suggested that there might be a difference in the charge states of the nuclear and cytoplasmic forms of CeHCF, due to either modification or association with other molecules. However, both these samples were active in forming VP16-induced complexes (Figure 4A, lane 15, and Figure 4C, lane 16). This active material was eluted between 0.4 and 0.9 M NaCl. Fractions containing the peak of VP16-induced complex activity from the cytoplasm were pooled and buffer exchanged using a desalting column without a loss of activity (Figure 4B, lanes 8 and 17). The CeHCF was further purified by anion-exchange chromatography on a Mono Q column. While CeHCF in nuclear extract eluted from the column directly (Figure 4A, lanes 8 and 16), in contrast the cytoplasmic CeHCF bound to the column and eluted between 0.15 and 0.25 M NaCl (Figure 4B, lanes 9 and 18). The flow-through of CeHCF from the nuclear extract was loaded on a cation-exchange column (Mono S), and the CeHCF activity was also present in the flow-through (data not shown). After concentration, the materials were subjected to gel filtration on Superdex HR-200. CeHCF from the nuclear extract or the cytoplasm migrated in a similar size range between 90 and 150 kDa (Figure 4A, lanes 9 and 17, Figure 4B, lanes 10 and 19, and data not shown). Finally, affinity chromatography on an anti-V5 agarose affinity gel resulted in further effective separation of CeHCF from other proteins. Analysis by SDS−PAGE showed that one major band migrated as the full-length CeHCF (Figure 4A, lane 5, and Figure 4B, lane 5), and this band reacted with the anti-SV5 antibody in a Western blot (Figure 4A, lane 10, and Figure 4B, lane 11). Three minor species with molecular masses between 45 and 70 kDa were also detected using anti-SV5 antibodies (Figure 4A, lane 10, and Figure 4B, lane 11).

The final affinity-purified CeHCF was capable of forming the VP16-induced complex (Figure 4A, lane 18, and Figure 4B, lane 20). The identity of the purified CeHCF was confirmed by MALDI mass spectrometry analysis of proteolytic digestion fragments. Mock cell lysates also followed the same purification procedure, but there were no detectable bands on the Western blot or VP16-induced complex activity in the gel retardation assay (Figure 4B, lane 21). Thus, our procedure was successful in the purification of CeHCF.

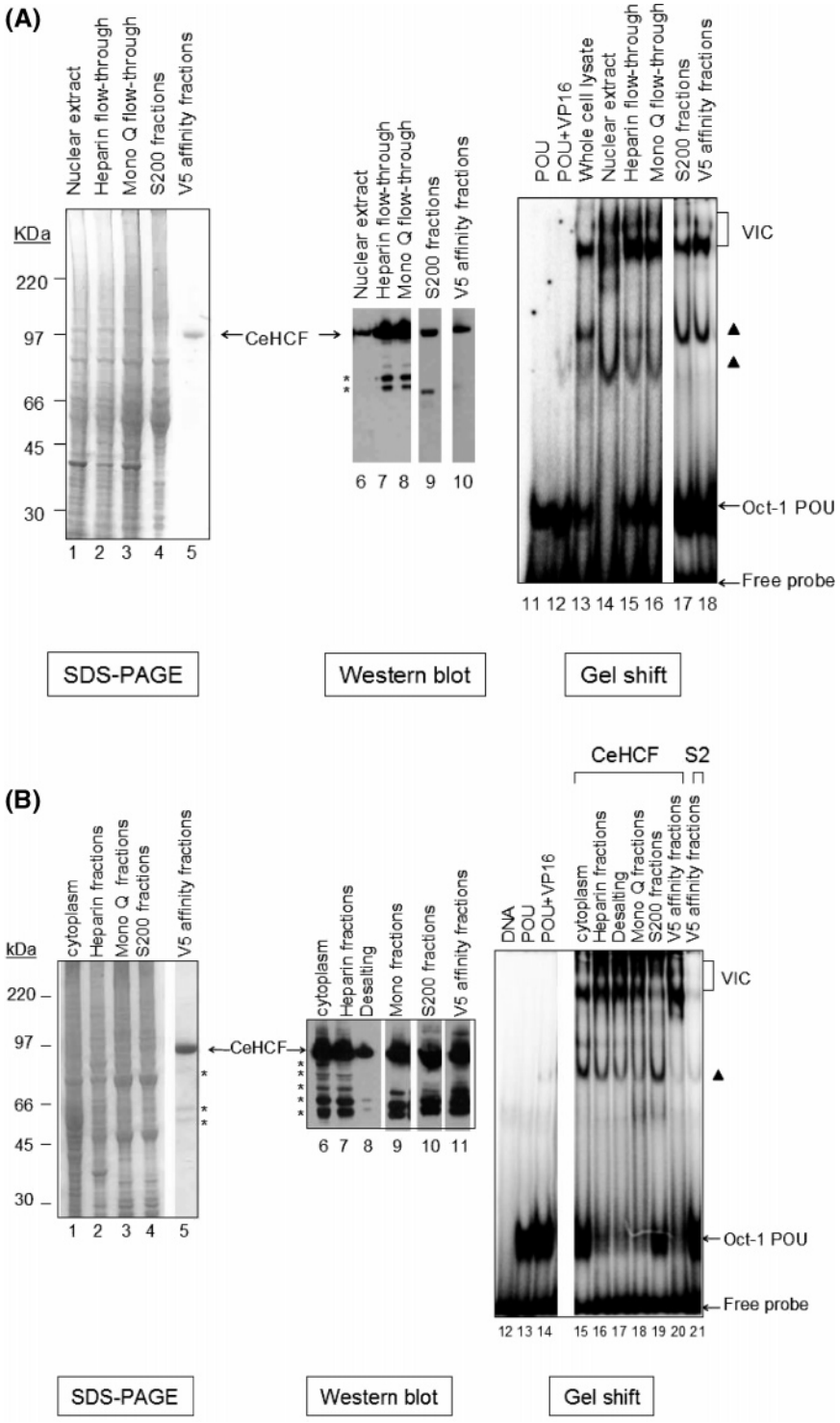

FIGURE 4: Enrichment and activity of the CeHCF during different purification steps. (A) Proteins from each step of purification were analyzed by SDS−PAGE (gel stained with Coomassie blue), by Western blotting, and by electrophoretic mobility shift assays for VP16-induced complex formation. The S2 cell nuclear extracts expressing CeHCF were isolated and tested (lanes 1, 6, and 14). The samples from immobilized heparin chromatography were in lanes 2, 7, and 15; ion-exchange chromatography on Mono Q (lanes 3, 8, and 16); size-exclusion chromatography on Superdex 200 (lanes 4, 9, and 17); and affinity column on an anti-V5 affinity gel (lanes 5, 10, and 18). The controls for the activity assay are shown in lanes 11−13, as described in the legend of Figure 2. (B) Cytoplasmic proteins of the S2 cell line stably expressing CeHCF were purified using procedures similar to those described for panel A. Samples were analyzed on a 4 to 12% SDS−PAGE gel (left panels), immunoblotted (middle panels), and tested via a gel retardation assay (right panels). The truncated CeHCF and nonspecific complex are indicated with asterisks and a triangle.

We also attempted to purify HCF-1(N380) and HCF-1(N411) expressed in *Drosophil*a S2 cells using the same purification procedure. However, the HCF fractions from the heparin column gradually lost their complex forming activity (data not shown).

HCF-1 and its interacting factors can be isolated from cell extracts using immobilized wheat germ agglutinin (WGA) (*22*), which interacts with proteins modified by O-linked *N*-acetylglucosamine residues. The CeHCF fraction was tested for interaction with WGA−agarose beads (Figure 5A).

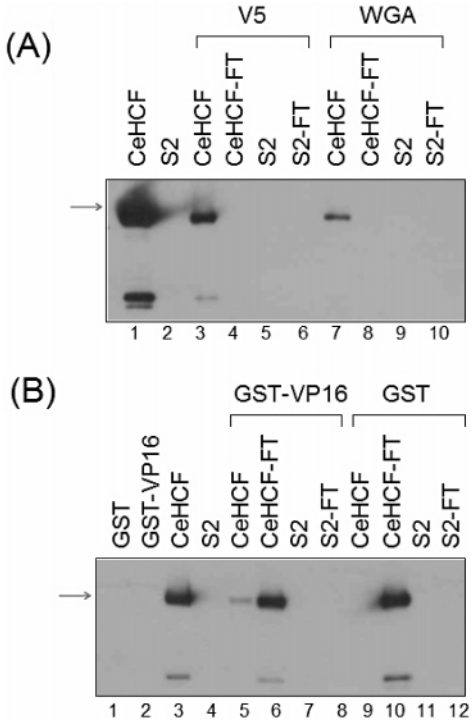

FIGURE 5: Interaction of CeHCF with wheat germ agglutinin and VP16. (A) Partially purified CeHCF was mixed with affinity agarose beads. A control extract was prepared by the same purification procedure from nonexpressing cells. After being washed, these beads and flow-through (FT) were analyzed by Western blotting using an anti-SV5−HRP antibody. The inputs were loaded in lanes 1 and 2 and samples of the beads in lanes 3, 5, 7, and 9; the flow-through was loaded in lanes 4, 6, 8, and 10. The proteins were incubated with anti-V5 agarose affinity gel shown in lanes 3−6; wheat germ agglutinin (WGA)−agarose beads were in lanes 7−10. (B) Partially purified CeHCF and control extract were incubated with the immobilized GST−VP16 fusion protein on glutathione−Sepharose (lanes 5−8) or with glutathione−Sepharose alone as a control (lanes 9−12). The prebead samples were loaded in lanes 3 and 4 and the binding beads in lanes 5, 7, 9, and 11; the flow-through was loaded in lanes 6, 8, 10, and 12. The purified GST and GST−VP16 fusion proteins were loaded in lanes 1 and 2. The bands corresponding to CeHCF are indicated with arrows.

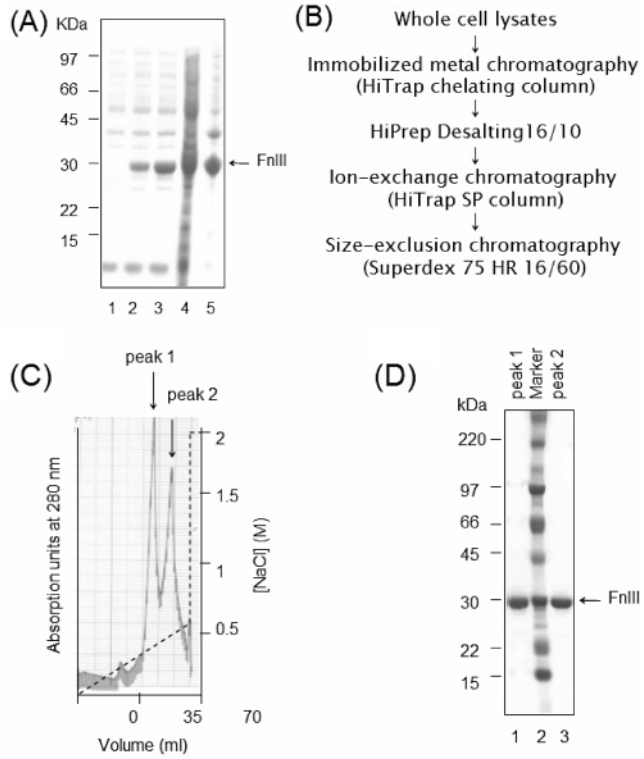

FIGURE 6: Expression and purification of the HCF-1 fibronectin domain (FnIII). (A) Time course of protein expression. The HCF-1(C1772) fusion protein was expressed in *E. coli*, and whole cell lysates from pre- and indicated post-induction were analyzed by SDS−PAGE (12% bisacrylamide gel). After a 2 h induction, the cells were harvested, sonicated, and clarified by centrifugation. The supernatant and pellet were applied in lanes 4 and 5, respectively. (B) Scheme for the purification of the HCF-1 FnIII domain. (C) HCF-1 FnIII domain separated into two peaks via ion-exchange chromatography. Whole cell lysates were first applied to immobilized metal chromatography and eluted with imidazole. The pooled fractions enriched in the HCF-1 FnIII domain were fractionated further with a HiTrap SP column into two species, peak 1 and peak 2. (D) Purity of the isolated HCF-1 FnIII domain as established by SDS−PAGE (lanes 1 and 3). The FnIII domain is indicated with arrowheads. Protein markers are in lane 2.

After being incubated and washed, the beads were analyzed by Western blotting, and a band with molecular mass of roughly 97 kDa was observed (lane 7). For comparison, the partially purified CeHCF, from the Superdex 200 fractionation of nuclear extracts, was purified with anti-SV5 agarose gels, and the beads and flow-through were probed with an anti-SV5−HRP antibody (Figure 5A). A major band corresponding to CeHCF was observed on the affinity beads (lane 3), while no detectable signal was in S2 cell lysates or its beads (lanes 5 and 6), or on beads mixed with the S2 cell lysates from mock expression controls (lanes 9 and 10).

To test if CeHCF can interact directly with VP16, pull-down assays were performed. CeHCF samples were incubated with glutathione−Sepharose that had bound the bacterially expressed GST−VP16 fusion protein. After being washed, the affinity beads and flow-through were analyzed via Western blotting using an anti-SV5−HRP antibody (Figure 5B), and a small amount of CeHCF was detected on the beads (lane 5). No band was seen using extracts from control S2 cells (lanes 4, 7, and 8). There was also no interaction between CeHCF and immobilized GST-bound glutathione−Sepharose (lane 9). These results indicate that the CeHCF produced from insect cells can interact directly with VP16.

Expression and Purification of the C-Terminal Fibronectin Type III-like Domain of Human HCF-1. Wilson et al. (*11*) reported that the smallest fragment of the C-terminal domain capable of HCF-1 self-association consisted of amino acid 1812−2002 (Figure 1). However, recombinant proteins encoding this smallest region were predominantly insoluble when expressed in *E. coli* (data not shown). An alternative construction was designed by considering the predicted secondary structure. A putative β-strand extends to residue 1772 toward the amino terminus, and residue 2005 is a lysine that is highly conserved in the HCF family. Therefore, we constructed a plasmid encompassing both these boundaries [residues 1772−2005, HCF-1(C1772)] (Figure 1B). Roughly 50% of HCF-1(C1772) was soluble in cell extracts (Figure 6A, lanes 4 and 5), which represents a significant improvement compared with the complete insolubility of the shorter construct (residues 1812−2002) (data not shown).

The soluble HCF-1(C1772) protein was extracted from a large-scale expression trial by metal affinity (Figure 6B) and cation-exchange chromatographies, which resulted in the fractionation of HCF-1(C1772) into two peaks [peak 1 and

peak 2 (Figure 6C)]. While the basis for the separation of C1772 into two peaks was not clear, the majority of the protein, whether from peak 1 or peak 2, further eluted during Superdex HR 75 column fractionation as a single peak at the expected size for a monomer (Figure 6D, lanes 1 and 3). Analysis by SDS−PAGE showed that these two proteins migrated to the same position, and MALDI fingerprinting corroborated their identity (data not shown). Electrospray ionization mass spectrometry analysis yielded a mass for peak 2 of 27 214.6 ± 1.5 Da, which is in good agreement with the expected mass of 27 215 Da for the processed form without an N-terminal methionine. The loss of the N-terminal methionine was corroborated by N-terminal sequencing. The mass of peak 1 was 27 387.1 ± 3.7 Da, and this could be attributed to the FnIII domain retaining the N-terminal methionine (expected mass of 27 347.1 Da) and carrying modifications, such as lysine methylation. We further characterized the peak 2 specimen, since it corresponds to the unmodified protein. Corroborating the observations from size-exclusion chromatography, we found the purified FnIII protein to be monomeric by analytical ultracentrifugation (results not shown).

The Fibronectin Type III-like Domain of Human HCF-1 Is Recruited into a VP16-Induced Complex. To examine the activity of the purified fibronectin domain of HCF-1, we assayed its interaction with the VP16-dependent complex formed using HCF-1(N411). The purified FnIII protein was able to form additional complexes of slower mobility that were not present in the controls (Figure 7A, lanes 3 and 4).

It was previously reported that the HCF N-terminal binding region of the FnIII domain is within residues 360−402 and that HCF-1(N380) is unable to associate with the C-terminus (*11*, *30*). Consistent with these findings, we observed no additional complex formation in the HCF-1(N380) reaction mixture in the presence of purified FnIII (Figure 7A, lanes 5 and 6).

Two complexes were observed with the HCF-1(N411) reaction mixture. To examine whether these complexes were related, the VP16-induced complex was titrated with purified FnIII proteins. However, the two complexes were induced coincidently, and thus, it is likely that they formed independently and represent different structures or oligomerization stages (results not shown). The FnIII was also recruited into a complex formed using the truncated version of VP16 that lacks the acidic C-terminal activation domain, and when titrated with FnIII showed a similar pattern of two independent supershifted species (Figure 7B). These results indicate that the negatively charged acidic activation region of VP16 does not play any role in stabilizing the recruitment of the fibronectin domain in the VP16-induced complex.

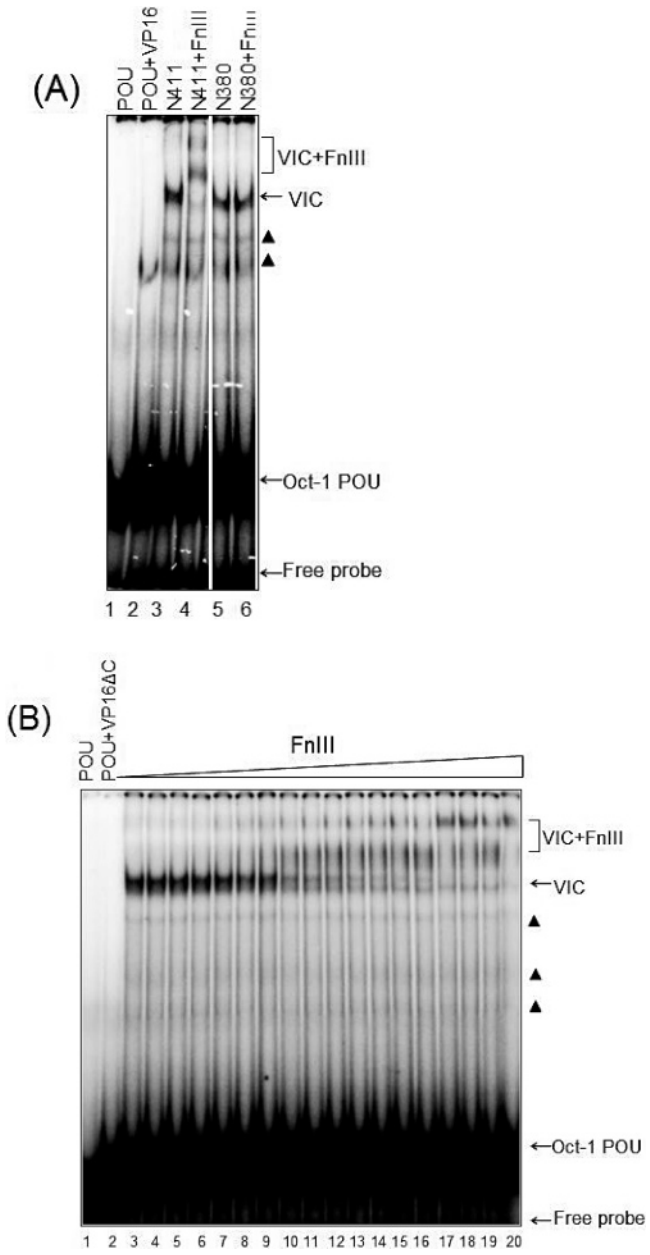

FIGURE 7: Formation of VP16-induced complexes with the FnIII domain of HCF-1. (A) The activity of the HCF-1 FnIII domain was tested with an electrophoretic mobility shift assay. The purified FnIII domain was incubated with whole cell lysates from S2 cells expressing HCF-1(N411) (lane 4) or HCF-1(N380) (lane 6), POU domain, and VP16. The control assays in the absence of the FnIII domain are shown in lanes 3 and 5. (B) A titration of the VIC with the FnIII domain. Whole lysates of HCF-1(N411) were mixed with various amounts of the purified FnIII domain, the POU domain, and the truncated VP16 (VP16ΔC) in lanes 3−20 (corresponding to 0, 10, 25, 50, 100, 200, 300, 400, 500, 600, 700, 800, 900, 1000, 1250, 1500, 1750, and 2000 ng of FnIII, respectively). Lanes 1 and 2 were controls as described in the legend of Figure 2. The positions of the VP16-induced complex alone or with the FnIII domain are indicated. The triangle marks a putative VP16−Oct1−DNA complex.

DISCUSSION

HCF plays an important role in activating intermediate early genes of HSV, and it has been implicated to function in cell proliferation, cytokinesis, and RNA splicing. However, due to the difficulties in the production of soluble materials on the scale of milligrams, the structures of HCF and of the VP16-induced complex are unknown. In this study, we have overexpressed the full-length HCF protein from *C. elegans* and the β-propeller and fibronectin domains from human HCF-1 for structural and functional characterization. Protocols for purifying the CeHCF and FnIII proteins were developed.

C. elegans HCF was observed to localize to the *Drosophila* S2 cell nucleus, whereas two truncated human HCFs [HCF-1(N380) and HCF-1(N411)] were entirely in the cytoplasm. Other studies have shown that a nuclear localization signal at the C-terminus of HCF is an important element for the

entry of protein into the nucleus. This might explain why the full-length CeHCF with a nuclear localization signal could enter the nucleus but the N-terminally truncated human HCF-1 without this element could not.

Earlier studies have shown that the *Drosophila* HCF is capable of supporting VP16-induced complex formation with the recombinant human Oct-1 POU domain on the TAATGARAT element (*34*). Similarly, the *C. elegans* HCF from crude extracts can also support an analogous cross-species complex of herpes simplex virus VP16, recombinant human Oct-1 POU domain, on the TAATGARAT element. Here, we show that the highly purified recombinant proteins are capable of forming the VIC, suggesting that these proteins alone are sufficient for the assembly and do not require any auxiliary factors or covalent modification. While such cross-species VP16-induced complexes are not likely to occur in nature, their stability in vitro suggests that they use common protein−protein and protein−DNA interfaces. Consistent with this proposal, *C. elegans* HCF was found to interact directly with VP16 in pull-down assays, which suggests that the HCF−VP16 interface is conserved. It might seem surprising that the HCF molecules from organisms such as flies and worms have conserved the ability of interacting with VP16, a protein from a human virus. This common association suggests that the interface that contacts VP16 must play an important conserved role in the cellular function of HCF.

In agreement with many earlier studies, the purified recombinant β-propeller domain of human HCF-1 was found to be capable of forming a "mini-VP16-induced complex" in the presence of recombinant Oct-1 POU and VP16. In this study, the fibronectin repeats of HCF-1 were also shown to be recruited into this mini-VP16-induced complex. This supershifted species was observed with the VIC formed with HCF-1(N411), but not with a smaller segment containing the proposed minimal region of the kelch domain (residues 2−380). This suggests that the recognition site of interaction of FnIII includes residues 380−411 in HCF-1. The result corroborates earlier studies showing that the fibronectin repeats interact with a segment that follows the minimal β-propeller domain (*11*), and it extends that earlier work by showing that the intramolecular interaction persists in the VP16-induced complex.

Two species resulted from the recruitment of the recombinant fibronectin domain into the VP16-induced complex. These appeared to form independently and may arise as a result of distinct stable conformations or, more likely, different fibronectin stoichiometry. Moreover, the negatively charged acidic activation region of VP16 does not play any role in stabilizing the recruitment of the fibronectin domain in the VP16-induced complex. We suggest that the VP16 activation domain and the fibronectin domain do not interact. However, the fibronectin domain could exert an indirect effect on transcriptional activation by recruiting other factors to the VIC. Testing the effect of this domain on the transcriptional activation properties of the VIC will be of interest. With the successful preparation of recombinant HCF-1 kelch and fibronectin domains and the full-length *C. elegans* HCF protein, further biochemical and biophysical analyses are now possible.

ACKNOWLEDGMENT

We thank Nick Gay and Jane Clarke for helpful advice. We thank Len Packman for mass spectrometry analysis and Charles Hill for synthesis of oligonucleotides.

REFERENCES

1. O'Hare, P. (1993) The virion transactivator of herpes simplex virus, *Semin. Virol. 4*, 145−155.
2. Herr, W. (1998) The herpes simplex virus VP16-induced complex: Mechanisms of combinatorial transcriptional regulation, *Cold Spring Harbor Symp. Quant. Biol. 63*, 599−607.
3. La Boissiere, S., Hughes, T., and O'Hare, P. (1999) HCF-dependent nuclear import of VP16, *EMBO J. 18*, 480−489.
4. Wilson, A. C., Freiman, R. N., Goto, H., Nishimoto, T., and Herr, W. (1997) VP16 targets an amino-terminal domain of HCF involved in cell cycle progression, *Mol. Cell. Biol. 17*, 6139−6146.
5. La Boissiere, S., Walker, S., and O'Hare, P. (1997) Concerted activity of host cell factor subregions in promoting stable VP16 complex assembly and preventing interference by the acidic activation domain, *Mol. Cell. Biol. 17*, 7108−7118.
6. Xue, F., and Cooley, L. (1993) Kelch encodes a component of intercellular bridges in *Drosophila* egg chambers, *Cell 72*, 681−693.
7. Adams, J., Kelso, R., and Cooley, L. (2000) The kelch repeat superfamily of proteins: Propellers of cell function, *Trends Cell Biol. 10*, 17−24.
8. Wilson, A. C., LaMarco, K., Peterson, M. G., and Herr, W. (1993) The VP16 accessory protein HCF is a family of polypeptides processed from a large precursor protein, *Cell 74*, 115−125.
9. Wilson, A. C., Peterson, M. G., and Herr, W. (1995) The HCF repeat is an unusual proteolytic cleavage signal, *Genes Dev. 9*, 2445−2458.
10. Kristie, T. M., Pomerantz, J. L., Twomey, T. C., Parent, S. A., and Sharp, P. A. (1995) The cellular C1 factor of the herpes simplex virus enhancer complex is a family of polypeptides, *J. Biol. Chem. 270*, 4387−4394.
11. Wilson, A. C., Boutros, M., Johnson, K. M., and Herr, W. (2000) HCF-1 amino- and carboxy-terminal subunit association through two separate sets of interaction modules: Involvement of fibronectin type 3 repeats, *Mol. Cell. Biol. 20*, 6721−6730.
12. Freiman, R. N., and Herr, W. (1997) Viral mimicry: Common mode of association with HCF by VP16 and the cellular protein LZIP, *Genes Dev. 11*, 3122−3127.
13. Lu, R., Yang, P., O'Hare, P., and Misra, V. (1997) Luman, a new member of the CREB/ATF family, binds to herpes simplex virus VP16-associated host cellular factor, *Mol. Cell. Biol. 17*, 5117−5126.
14. Lu, R., Yang, P., Padmakumar, S., and Misra, V. (1998) The herpesvirus transactivator VP16 mimics a human basic domain leucine zipper protein, Luman, in its interaction with HCF, *J. Virol. 72*, 6291−6297.
15. Lu, R., and Misra, V. (2000) Zhangfei: A second cellular protein interacts with herpes simplex virus accessory factor HCF in a manner similar to Luman and VP16, *Nucleic Acids Res. 28*, 2446−2454.
16. Mahajan, S. S., Little, M. M., Vazquez, R., and Wilson, A. C. (2002) Interaction of HCF-1 with a cellular nuclear export factor, *J. Biol. Chem. 277*, 44292−44299.
17. Vogel, J. L., and Kristie, T. M. (2000) The novel coactivator C1 (HCF) coordinates multiprotein enhancer formation and mediates transcription activation by GABP, *EMBO J. 19*, 683−690.
18. Gunther, M., Laithier, M., and Brison, O. (2000) A set of proteins interacting with transcription factor Sp1 identified in a two-hybrid screening, *Mol. Cell. Biochem. 210*, 131−142.
19. Piluso, D., Bilan, P., and Capone, J. P. (2002) Host cell factor-1 interacts with and antagonizes transactivation by the cell cycle regulatory factor miz-1, *J. Biol. Chem. 277*, 46799−46808.
20. Ajuh, P., Browne, G. J., Hawkes, N. A., Cohen, P. T., Roberts, S. G., and Lamond, A. I. (2000) Association of a protein phosphatase 1 activity with the human factor C1 (HCF) complex, *Nucleic Acids Res. 28*, 678−686.
21. Scarr, R. B., and Sharp, P. A. (2002) PDCD2 is a negative regulator of HCF-1 (C1), *Oncogene 21*, 5245−5254.
22. Wysocka, J., Myers, M. P., Laherty, C. D., Eisenman, R. N., and Herr, W. (2003) Human Sin3 deacetylase and trithorax-related

Set1/Ash2 histone H3−K4 methyltransferase are tethered together selectively by the cell-proliferation factor HCF-1, *Genes Dev. 17*, 896−911.

23. Wysocka, J., Reilly, P. T., and Herr, W. (2001) Loss of HCF-1-chromatin association precedes temperature-induced growth arrest of tsBN67 cells, *Mol. Cell. Biol. 21*, 3820−3829.
24. Goto, H., Motomura, S., Wilson, A. C., Freiman, R. N., Nakabeppu, Y., Fukushima, K., Fujishima, M., Herr, W., and Nishimoto, T. (1997) A single-point mutation in HCF causes temperature-sensitive cell-cycle arrest and disrupts VP16 function, *Genes Dev. 11*, 726−737.
25. Julien, E., and Herr, W. (2003) Proteolytic processing is necessary to separate and ensure proper cell growth and cytokinesis functions of HCF-1. *EMBO J. 22*, 2360−2369.
26. Johnson, K. M., Mahajan, S. S., and Wilson, A. C. (1999) Herpes simplex virus transactivator VP16 discriminates between HCF-1 and a novel family member, *J. Virol. 73*, 3930−3940.
27. Liu, Y., Hengartner, M. O., and Herr, W. (1999) Selected elements of herpes simplex virus accessory factor HCF are highly conserved in *Caenorhabditis elegans*, *Mol. Cell. Biol. 19*, 909−915.
28. Lee, S., and Herr, W. (2001) Stabilization but not the transcriptional activity of herpes simplex virus VP16-induced complexes is evolutionarily conserved among HCF family members, *J. Virol. 75*, 12402−12411.
29. Izeta, A., Malcomber, S., O'Rourke, D., Hodgkin, J., and O'Hare, P. (2003) A C-terminal targeting signal controls differential compartmentalisation of *Caenorhabditis elegans* host cell factor (HCF) to the nucleus or mitochondria, *Eur. J. Cell Biol. 82*, 495−504.
30. Hughes, T. A., La Boissiere, S., and O'Hare, P. (1999) Analysis of functional domains of the host cell factor involved in VP16 complex formation, *J. Biol. Chem. 274*, 16437−16443.
31. Gay, N. J., Poole, S., and Kornberg, T. (1988) Association of the *Drosophila melanogaster* engrailed protein with specific soluble nuclear protein complexes, *EMBO J. 7*, 4291−4297.
32. Grossmann, J. G., Sharff, A. J., O'Hare, P., and Luisi, B. (2001) Molecular shapes of transcription factors TFIIB and VP16 in solution: Implications for recognition, *Biochemistry 40*, 6267−6274.
33. Chang, J. F., Phillips, K., Lundback, T., Gstaiger, M., Ladbury, J. E., and Luisi, B. (1999) Oct-1 POU and octamer DNA co-operate to recognise the Bob-1 transcription co-activator via induced folding, *J. Mol. Biol. 288*, 941−952.
34. Mahajan, S. S., Johnson, K. M., and Wilson, A. C. (2003) Molecular cloning of *Drosophila* HCF reveals proteolytic processing and self-association of the encoded protein, *J. Cell. Physiol. 194*, 117−126.

BI050357L